Environ. Sci. Technol. **2006**, *40,* 5943−5949

Hyporheic Exchange and Fulvic Acid Redox Reactions in an Alpine Stream/Wetland Ecosystem, Colorado Front Range

MATTHEW P. MILLER,*,† DIANE M. MCKNIGHT,† ROSE M. CORY,† MARK W. WILLIAMS,‡ AND ROBERT L. RUNKEL§

Department of Civil, Environmental, and Architectural Engineering, Institute of Arctic and Alpine Research, University of Colorado, Boulder, Colorado 80309-0450, and Department of Geography, Institute of Arctic and Alpine Research, University of Colorado, Boulder, Colorado 80309-0450, and U.S. Geological Survey, Denver, Colorado 80225

The influence of hyporheic zone interactions on the redox state of fulvic acids and other redox active species was investigated in an alpine stream and adjacent wetland, which is a more reducing environment. A tracer injection experiment using bromide (Br^-) was conducted in the stream system. Simulations with a transport model showed that rates of exchange between the stream and hyporheic zone were rapid ($\alpha \approx 10^{-3}$ s^{-1}). Parallel factor analysis of fluorescence spectra was used to quantify the redox state of dissolved fulvic acids. The rate coefficient for oxidation of reduced fulvic acids ($\lambda = 6.5 \times 10^{-3}$ s^{-1}) in the stream indicates that electron-transfer reactions occur over short time scales. The rate coefficients for decay of ammonium ($\lambda = 1.2 \times 10^{-3}$ s^{-1}) and production of nitrate ($\lambda = -1.0 \times 10^{-3}$ s^{-1}) were opposite in sign but almost equal in magnitude. Our results suggest that fulvic acids are involved in rapid electron-transfer processes in and near the stream channel and may be important in determining ecological energy flow at the catchment scale.

Introduction

Fluxes of dissolved organic carbon (DOC) in mountain catchments of the western United States vary with hydrograph stage (*1*, *2*) and inter-annual climate variation (*3*). Further, chemical characterization of DOC has shown that, in stream systems without lakes, DOC is derived primarily from humified terrestrial material flushed into the stream, especially during spring snowmelt (*4*, *5*). In contrast, in catchments that contain lakes, a substantial portion of the DOC is derived from lacustrine algal production, especially during summer (*6*). Moreover, DOC and nitrogen (N) cycling appear to be coupled in these catchments (*7*−*9*).

As observed in many small catchments, both DOC and N dynamics may be influenced by hyporheic zone interactions (*10*−*12*). Production of fulvic acids through degradation of plant biomass in surrounding uplands and wetlands can enhance concentrations of dissolved fulvic acids in the hyporheic zone (*2*), and the transport of fulvic acids to the stream by hyporheic exchange. In addition to a DOC gradient between the hyporheic zone and the stream, there is typically a redox gradient with greater concentrations of reduced chemical species (*10*) in the hyporheic zone. Although the influence of hyporheic interactions on the redox chemistry of N species (*10*−*12*) has been studied, the influence of hyporheic exchange on fulvic acid redox chemistry has not been investigated.

Advances in fluorescence spectroscopy of fulvic acids have the potential to provide insight into redox reactions in hyporheic zones. In natural waters, including those examined in this study, fulvic acids are the dominant fraction of humic substances (*7*). The quinone moieties of dissolved fulvic acids that are primarily responsible for their electron accepting capacity have fluorescent properties, allowing for the characterization of the redox state of the fulvic acid fraction of dissolved organic matter (DOM) at natural concentrations (*13*−*16*). Laboratory studies have demonstrated that the redox state of fulvic acid quinone moieties change through microbial reduction and interaction with iron and other redox active species (*17*, *18*).

This study focuses on quantifying the redox state and rates of oxidation/reduction of fulvic acids in the hyporheic zone and the main stream channel of an alpine stream with an adjacent wetland. Our approach was to quantify rates of hyporheic exchange by conducting a conservative tracer experiment and to determine the concentrations of redox active species at stream and hyporheic zone sites. The steps taken were (1) to quantify the magnitude of hyporheic exchange; (2) to examine changes in concentrations of redox-active species between the stream and hyporheic zone, including fulvic acids, ammonium (NH_4^+), nitrate (NO_3^-), and iron (Fe); (3) to quantify rates of redox reactions associated with hyporheic exchange, and (4) to evaluate the importance of hyporheic exchange using a two-component mixing model at the catchment scale. The results show that hyporheic zone interaction influences the oxidation state of dissolved fulvic acids, as well as that of other redox active species. Furthermore, the results suggest that hyporheic exchange is an important process in determining energy flow (i.e., electron transport in ecosystems) at the catchment scale.

Materials and Methods

Site Description. The research site is the upper Green Lakes Valley, a glacial valley on the Continental Divide in the Colorado Front Range. Green Lakes Valley is within the Silver Lake Watershed, which provides 40% of the water supply for Boulder, Colorado. The Niwot Ridge Long-Term Ecological Research project (NWTLTER) has conducted climatic, water quality, and biological studies at this site for 50 years (*19*). The 9-ha Arikaree Glacier (ARK) is at the head of the valley directly above the Navajo Stream (NAV) site, which forms the headwaters of North Boulder Creek (Figure 1). NAV is a braided first-order stream located on a "shelf" above Green Lake 5 (GL5) at an elevation of 3750 m. The 50-m NAV study reach has a steep talus slope on the north side and a shallow alpine wetland on the south side, which was saturated to the surface during July 2003.

Field Methods. The NAV stream reach was divided into three sub-reaches with sampling sites located 15 m (S1), 22 m (S2), and 42 m (S3) below the injection site (Figure 1). A tributary entered the stream between sites S1 and S2. Sixteen

* Corresponding author phone: (303) 735-2495; fax: (303) 492-6388; e-mail: Matthew.P.Miller-1@Colorado.edu.

† Department of Civil, Environmental, and Architectural Engineering, Institute of Arctic and Alpine Research, University of Colorado, Boulder.

‡ Department of Geography, Institute of Arctic and Alpine Research, University of Colorado, Boulder.

§ U.S. Geological Survey.

10.1021/es060635j CCC: $33.50
Published on Web 08/23/2006

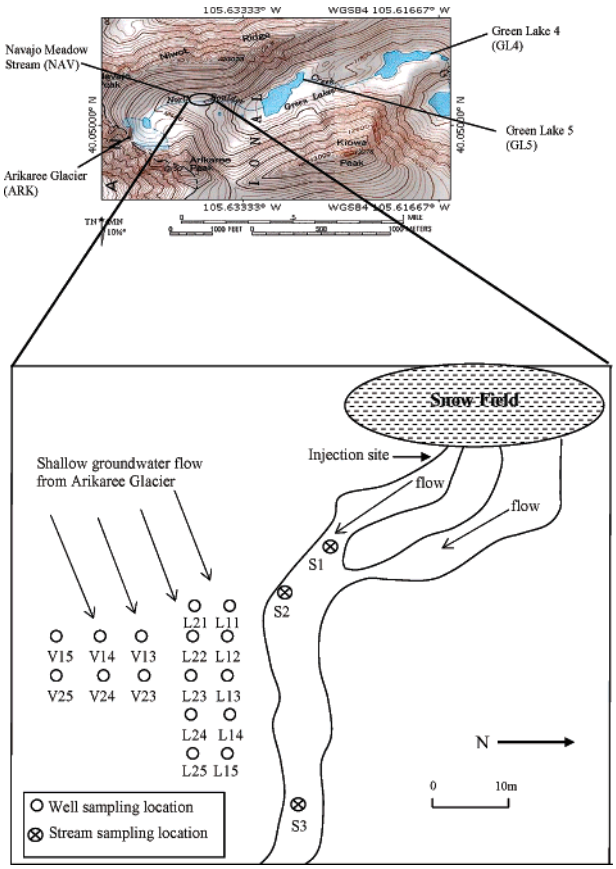

FIGURE 1. Schematic map of the Navajo Meadow Stream and surroundings showing the sampling locations for the tracer injection experiment.

wells of 30−35 cm depth were dug as small pits located adjacent to reach 3 in rows both parallel and perpendicular to the direction of flow (Figure 1, Table S1). Water samples were collected from stream and well sites on 10, 17, and 24 July, 2003. Samples for analysis of DOC, Fe, oxygen isotopes ($\delta^{18}O$), and fluoresence spectroscopy were collected in precombusted 60 mL amber glass bottles and filtered on site with pre-combusted 1.2 μm, 47-mm Whatman glass-fiber filters with a hand-pump filtration system. Samples for analysis of major ions, NH_4^+, and NO_3^- were collected in 250 mL Nalgene HDPE bottles, and filtered with 1 μm, 47 mm Gelman A/E glass-fiber filters. All samples were stored at 4 °C. The ARK, Green Lake 4 (GL4) and NAV (S3 stream site) sites are sampled weekly from snowmelt through the summer for major solutes, nutrients, and isotopes by the NWTLTER program (http://culter.colorado.edu).

A constant-injection experiment using bromide (Br^-) as a conservative tracer was conducted on 10 July 2003. A 0.1 M solution of lithium bromide (LiBr) was injected into the stream at a constant rate of 1 L min^{-1} from 1207 to 1256 h. Stream sites were sampled every 5−10 min before, during, and for 2 h after the injection of the tracer. Well samples were taken approximately once every half hour. All sites were sampled once on the following day. Samples for Br^- analysis were filtered on site using 0.4 μm GeoFilters and collected in 60 mL Nalgene HDPE bottles.

Laboratory Analysis. Analyses for Br^-, NO_3^-, and NH_4^+ followed protocols of the NWTLTER project. Br^- concentrations were analyzed using a Metrohm 761 compact ion chromatograph with a Metrosep A Supp 250 × 4 mm column with a detection limit of 0.001 mg L^{-1} and a precision of 0.26%. NH_4^+ and NO_3^- were analyzed by ion chromatography with detection limits of 0.28 μeq/L and 0.02 μeq L^{-1} and precisions of 3.3% and 0.73%, respectively. DOC concentrations were measured with a Shimadzu TOC-550A total organic carbon analyzer, with a confidence interval of 0.02 mg L^{-1}. Acidified samples were analyzed for total dissolved iron on an AAnalyst 100 atomic absorption spectrometer, with a confidence interval of 0.02 mg L^{-1}. Analysis of all samples for $\delta^{18}O$ was done at the Stable Isotope Laboratory at INSTAAR (*20*). The 1-σ precision was ± 0.05 ‰.

Fluorescence Characteristics of DOM. Three-dimensional fluoresence scans were run on filtered whole water samples using a JY-Horiba/Spex Fluoromax-2 spectrofluorometer with DataMax data acquisition software. Scans were corrected for excitation and emission in Matlab (*21*). The fluorescence index (FI) was calculated for each sample (*5*), and the standard deviation associated with triplicate analyses was 0.01 (*7*). Given that the saturated conditions in the wetland would have resulted in some atmospheric exposure, samples for fluorescence analysis were filtered immediately upon collection but not processed in an anoxic environment. Studies have found that reduced quinones can be stable without precautions taken to limit oxygen exposure (*14*, *17*). Parallel factor analysis (PARAFAC) was used to characterize the fluorescent fraction of the DOM. PARAFAC corresponds to a three-way version of principal component analysis, and when applied to the excitation−emission matrices (EEMs) of samples containing DOM, identifies different classes of fluorophores, herein referred to as "components" (*16*). An EEM can be represented as a sum of the components. The 54 EEMs from this study were included in the 379 EEMs analyzed with PARAFAC as part of the model run presented in Cory and McKnight (*15*) (Figure S1). Of the 13 components, three components (Q1, Q2, and Q3) were identified as being quinone-like, three (SQ1, SQ2, and SQ3) as similar to semiquinones, and one (HQ) as being hydroquinone-like (*15*). We represented the differences in the oxidation state of fulvic acids by the following redox index (RI):

$$\mathrm{RI} = \frac{Q_{\mathrm{red}}}{(Q_{\mathrm{red}} + Q_{\mathrm{ox}})} \quad (1)$$

where Q_{red} is the sum of the loadings of the reduced components (SQ1, SQ2, SQ3, and HQ), and Q_{ox} is the sum of the loadings of the oxidized, quinone-like components (Q1, Q2, and Q3). A modeled EEM at S3 assuming conservative transport of all PARAFAC components was created using Matlab.

Solute Transport Modeling. Solute transport modeling was used to (1) quantify hyporheic exchange, and (2) quantify the production and loss of reactive chemical constituents. For small, narrow streams such as NAV, solute transport is often quantified by modeling transient storage (*22*), which refers to the temporary detainment of solutes in small eddies and stagnant open-water areas of the channel (surface storage), and the exchange of water between the channel and the porous media adjacent to the channel (hyporheic exchange). Due to the relatively narrow stream channel, surface storage in NAV is negligible and transient storage is dominated by hyporheic exchange. Transient storage was modeled using OTIS (one-dimensional transport with inflow and storage, ref *23*), which considers advection, dispersion, inflow, and storage. In addition, the production and loss of reactive constituents may be considered. Within OTIS, constituent concentrations in the main channel (C) and the storage zone (C_S) are given by the following:

$$\frac{\partial C}{\partial t} = -\frac{Q}{A}\frac{\partial C}{\partial x} + \frac{1}{A}\frac{\partial}{\partial x}\left(AD\frac{\partial C}{\partial x}\right) + \frac{q_{\mathrm{LIN}}}{A}(C_{\mathrm{L}} - C) + \alpha(C_{\mathrm{S}} - C) - \lambda C \quad (2)$$

$$\frac{dC_s}{dt} = \alpha\frac{A}{A_s}(C - C_S) - \lambda_s C_s \quad (3)$$

where A is the main channel cross-sectional area [m^2], A_s is the storage zone cross-sectional area [m^2], C_L represents the lateral inflow solute concentration [mg L^{-1}], D is the dispersion coefficient [m^2 s^{-1}], Q is the volumetric flow rate [m^3 s^{-1}], q_{LIN} is the lateral inflow rate [m^3 (s-m)$^{-1}$], t is time [s], x is distance [m], α is the storage zone exchange coefficient [s^{-1}], and λ and λ_s represent the main channel and storage zone first-order decay coefficients, respectively [s^{-1}]. The hydrologic processes governing constituent transport in NAV were quantified using data from the conservative Br^- tracer (Supporting Information, Section 1). The transport of reactive constituents (DOC, RI, NH_4^+, and NO_3^-) from S2 to S3 was quantified using the observed data and the steady-state solution of the governing equations (eqs 2 and 3 with the left-hand-side set equal to zero) (Supporting Information, Section 2). Model parameters were used to calculate the fraction of median travel time attributed to hyporheic exchange as follows (*24*):

$$F_{med} = (1 - e^{-L(\alpha/\mu)})\frac{A_s}{A + A_s} \quad (4)$$

where L is the downstream distance (m) and μ is advective velocity (m s^{-1}). When normalized to a reach length of 200 m (F_{med}^{200}) values in other stream systems range from 0.0012 to 0.6801 with a median value of 0.0532 (*24*).

Two-Component Mixing Model. Discharge in the NAV reach (measured at the S3 site from the tracer injection experiment) was separated into new and old water components using $\delta^{18}O$ with a two-component mixing model as described for GL4 (*25*) (Supporting Information, Section 3).

Results

Analysis of Dissolved Constituents. Significant differences exist between the average values of DOC, FI, RI, Fe, NH_4^+, and NO_3^-, at the stream and well sites (Table S2). The results of a two-sample t-test for the two-tailed hypothesis show that the DOC was significantly lower in the stream (0.5 mg L^{-1}) compared to the wells (2.1 mg L^{-1}) ($p < 0.05$) by a factor of 4. The FI in the stream of 1.50 was significantly higher than the FI of 1.35 for the wells ($p < 0.05$). The RI in the stream (0.39) was lower than in the wells (0.51) ($p < 0.05$). Higher values of FI correspond to a greater contribution of microbial sources of fulvic acid and higher RI corresponds to more reduced fulvic acid species. Fe shows a similar trend with lower values in the stream (0.19 mg L^{-1}) compared with the wells (0.24 mg L^{-1}) ($p < 0.05$). The NH_4^+ was significantly lower in the stream (1.23 μeq L^{-1}) compared to the wells (2.54 μeq L^{-1}) ($p < 0.05$). In contrast, NO_3^- was greater, by a factor of 3, in the stream (19.3 μeq L^{-1}) compared to the wells (6.0 μeq L^{-1}) ($p < 0.05$).

Stream Tracer Experiment. The Br^- concentrations in stream and well waters prior to injection were below the detection limit of 0.001 mg L^{-1} (Figure 2). During the experiment, Br^- concentrations increased rapidly and then remained relatively constant at about 2.8 mg L^{-1} at S1 and about 1.9 mg L^{-1} at S3. There was a rapid return to pre-injection levels after the injection ceased. Calculated discharge at S3 was 8.1×10^{-2} m^3 s^{-1}. The groundwater contribution to streamflow for this reach was 7.3×10^{-3} m^3 s^{-1}, or about 10% of discharge at S3 (Supporting Information, Section 1). The Br^- concentrations in the wells ranged from below detection to 0.73 mg L^{-1}. Br^- was detected in well sites for up to 19 h after the conclusion of the tracer injection.

The OTIS-P simulations for Br^- concentrations at the two stream sites match well with the measured Br^- concentrations (Figure 2). The model accurately simulated an intermediary point on the rising limb for both reaches. Parameter estimates for the main channel cross sectional area, A, are within 5% of the measured values at S1 and S3 (0.18 and 0.21 m^2 respectively) (Table 1). A_s is smaller than A in reach 1 and greater than A in reach 3 by a factor of 4. Parameter estimates

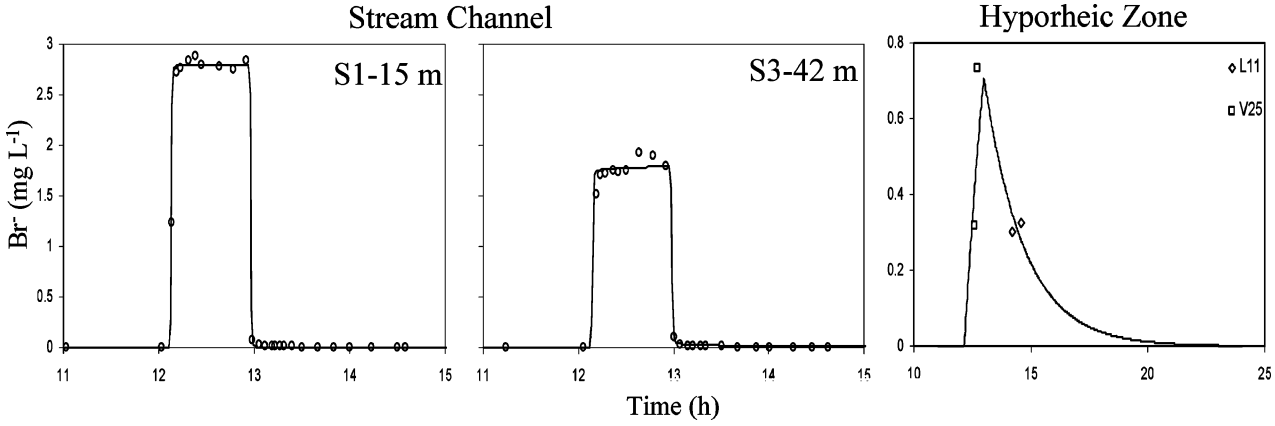

FIGURE 2. OTIS simulated ion of Br^- concentrations (lines) at the S1 stream site (15 m downstream of the injection site), the S3 stream site (42 m downstream of the injection site), and in the hyporheic zone compared to measured Br^- concentrations (symbols).

TABLE 1. Calculated Parameter Values from the Bromide Transport Simulation.[a]

reach	X (m)	Q (m^3 s^{-1})	q_{LIN} (m^3 s^{-1} m^{-1})	D (m^2 s^{-1})	A(m^2)	A_s(m^2)	A_s/A	α (s^{-1})
1	15.5	0.053	0.00	0.5	0.17	0.03	0.18	2.2×10^{-3}
2	6.4	0.073	2.9×10^{-3}	0.8	0.21	0.87	4.1	7.1×10^{-4}
3	20.8	0.081	3.5×10^{-4}	0.8	0.21	0.87	4.1	7.1×10^{-4}

	λ_{DOC}	λ_{sDOC}	λ_{RI}	λ_{sRI}	λ_{NH4+}	λ_{sNH4+}	λ_{NO3-}	λ_{sNO3-}
3	1.6×10^{-2}	-1.3×10^{-4}	6.5×10^{-3}	-8.4×10^{-5}	1.2×10^{-3}	-7.9×10^{-5}	-1.0×10^{-3}	1.0×10^{-4}

[a] Also shown are in-stream and hyporheic production/decay terms used to simulate reactive transport (negative values indicate production and positive values indicate decay).

for α are approximately 1×10^{-3} s^{-1}, indicating high rates of exchange. The F_{med}^{200} was 0.25 which is greater than the median value by a factor of 5. There was a good match between the simulated storage zone Br^- concentrations in reach 3 and the observed concentrations in the four wells that had Br^- concentrations greater than 0.2 mg L^{-1}(Figure 2).

The steady-state analysis provided insight into the reactivity of redox active species. First, the simulation showed that measured DOC, RI, NH_4^+, and NO_3^- concentrations deviated from simulated concentrations assuming conservative transport (i.e., no reactions in the stream or hyporheic zone) (Figure 3). For the first-order rate coefficients used to simulate reactive transport in the main channel and storage zone (Table 1), negative values indicate production and positive values indicate decay. The rate coefficient for the loss of DOC in the stream ($\lambda = 1.6 \times 10^{-2}$ s^{-1}) is an order of magnitude greater than any of the other rate coefficients. The rate coefficient for the decay of RI ($\lambda = 6.5 \times 10^{-3}$ s^{-1}), corresponding to the oxidation of fulvic acids, is the same order of magnitude as the rate coefficient for the decay of NH_4^+ ($\lambda = 1.2 \times 10^{-3}$ s^{-1}). The rate coefficients for decay of NH_4^+ and production of NO_3^- ($\lambda = -1.0 \times 10^{-3}$ s^{-1}) are opposite in sign but almost equal in magnitude. Although it is not possible to calculate rate coefficients for the stream system on sampling dates when a tracer injection experiment was not conducted, the discharge and chemical concentrations on 17 and 24 July were similar to those on 10 July.

Figure 4 compares the measured EEM and the PARAFAC modeled EEM at S3 from the day of the tracer experiment with the modeled EEM at S3 assuming conservative transport of all fluorescent components. The conservative transport EEM shows clearly resolved peaks with greater intensity in the region of the EEM that is associated with fulvic acid peaks (*26*). The RI of the measured EEM was 0.39 compared to 0.54 for the conservative transport EEM.

Chemical and Isotopic Content of Stream Waters at the Catchment Scale. The DOC concentrations at all sites were highest on the rising limb of the hydrograph and then decreased (Figure 5a). A paired-difference t-test shows no significant difference ($p > 0.05$) in the concentrations of DOC between the NAV site and the outflow to GL4. NO_3^- concentrations show a similar pattern, with high concentrations on the rising limb of the hydrograph, and seasonally low concentrations during the summer months (Figure 5b). During the summer, NO_3^- concentrations at NAV were approximately twice those of ARK. A paired-difference t-test shows that NO_3^- concentrations were significantly higher ($p < 0.05$) at NAV than at the ARK outlet. NH_4^+ concentrations were greatest before the initiation of spring snowmelt and then decreased as the summer progressed (Figure 5c). A paired-difference t-test shows that NH_4^+ concentrations at the outflow of ARK were significantly higher than at the NAV or GL4 sites ($p < 0.05$).

The $\delta^{18}O$ content of all three sites was most depleted at the initiation of snowmelt and became progressively more enriched with time (Figures 5d, 5e). Values from NAV and the GL4 outlet were generally 1−1.5 ‰ more enriched than outflow from ARK. The two-component mixing model shows that "old" water composed about 20% of surface flow at NAV site during July and then gradually increased to near 100% with baseflow conditions in autumn.

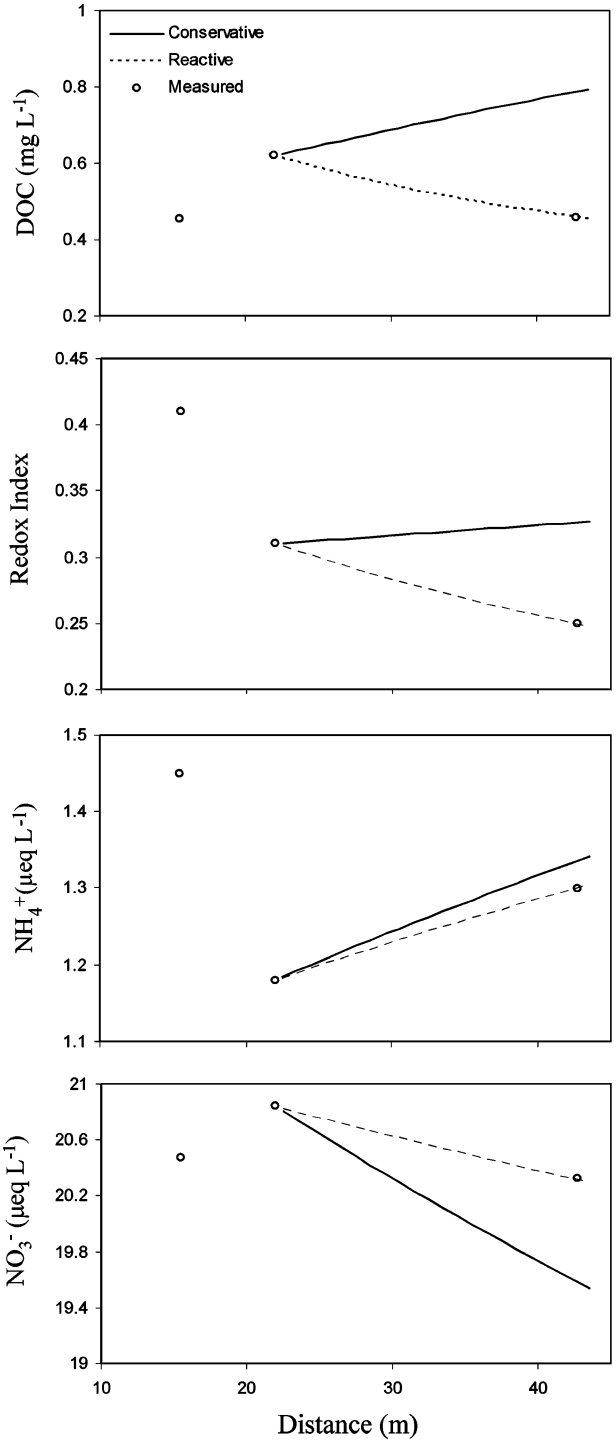

FIGURE 3. Observed (symbols), conservative simulation (solid line), and reactive simulation (dashed line) data for DOC, the redox index (RI), NH_4^+, and NO_3^- at S1, S2, and S3 on the day of the tracer injection experiment. As the summer progressed, variation between stream sites decreased. Conservative and reactive transport simulations are shown for the third reach only due to the location of the wells (see Figure 1).

Discussion

Hyporheic exchange was a significant component of streamflow at NAV. This is indicated by the F_{med}^{200} of 0.25, which is on the upper end of the range of reported values (*24*). Main channel cross-sectional areas, as well as lateral inflow values and dispersion coefficients, are of the same order of magnitude as those reported for other mountain streams (*27*, *28*). The storage zone areas of ~ 0.9 m^2 fall within the range for high-gradient streams (*29*) and exchange coefficients ($\alpha \approx 10^{-3}$ s^{-1}) fall on the high end of the range for other mountain streams (*24*, *30*). Both the in-stream and storage zone simulations matched well with the observed Br^- concentrations. For those wells close to the stream, the sampling at approximately 0.5 h intervals may not have been frequent enough to catch the maximum Br^- in the pulse.

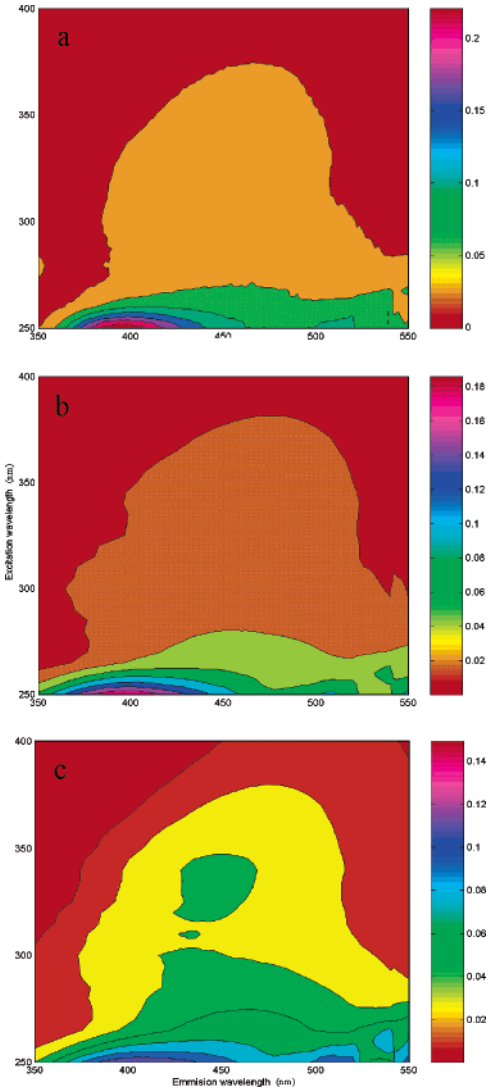

FIGURE 4. Comparison of (a) the measured EEM at S3 on the day of the tracer experiment with (b) the PARAFAC model output of the EEM at S3 and (c) the modeled EEM at S3 simulated using OTIS and assuming conservative transport of all PARAFAC components. Intensities in Raman Units (RU).

The large Br^- concentrations observed in well V25 in comparison with wells closer to the stream may reflect longer flow paths in the hyporheic zone that do not run parallel to the stream channel. The presence of Br^- in the hyporheic zone for up to 19 h following the tracer injection provides further evidence that there was substantial interaction between the saturated porous wetland and the stream channel. This observation, in combination with the high rates of exchange, indicates that there was significant transport of redox active species into and out of the hyporheic zone in the study reach.

Distinct differences were found in the concentrations of redox active species between the stream and the wetland. The presence of reduced fulvic acids (RI) was more pronounced in the wetland. Moreover, differences in RI were associated with differences in dominant inorganic N species. The prevalence of reducing conditions and reduced fulvic acid species in the wetland may explain the greater iron concentrations in the wetland as compared to the stream because the measured soluble iron in the wetland may have been predominantly ferrous iron.

Quantification of the rate coefficients for production and decay of the reactive constituents links the chemical differences between the two sites to hydrologic transport processes. Deviation of concentrations of reactive constituents simulated assuming conservative transport from the reactive–transport concentrations is evidence that reactions taking place in the hyporheic zone are important controls on in-stream concentrations. Reactive transport simulations indicate that the wetland is a source of reduced fulvic acids and NH_4^+ while these constituents are oxidized in the main stream channel. The nearly identical rate coefficients for decay of NH_4^+ and production of NO_3^- in the stream suggest that NH_4^+ is rapidly oxidized to NO_3^-. These results are

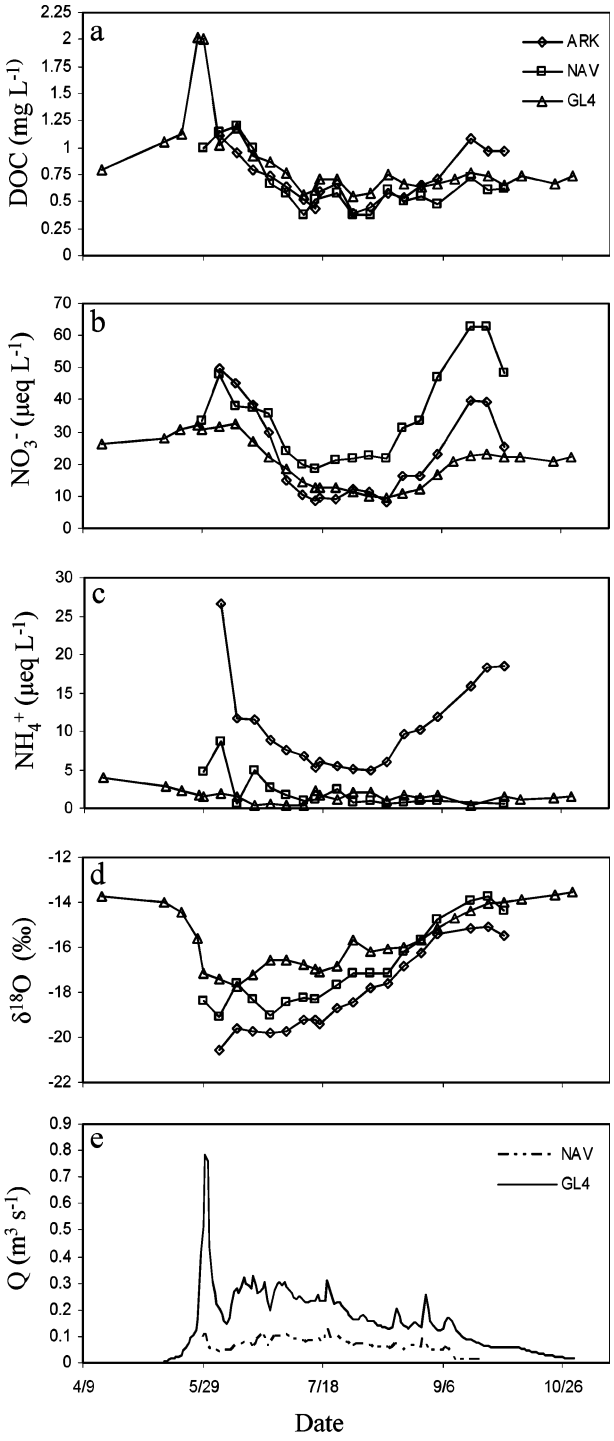

FIGURE 5. Streamwater concentrations of DOC, NO_3^-, NH_4^+, and $\delta^{18}O$ (a-d) at the outflow of the Arikaree Glacier (ARK), the Navajo stream site (NAV), and the outlet of Green Lake 4 (GL4). Also shown are the hydrographs for the NAV and GL4 sites (e).

consistent with the previously observed trend that the most rapid uptake of NH_4^+ and transformation to NO_3^- occurred in the smallest streams (*31*).

Our results suggest that fulvic acids may be similarly involved in electron-transfer processes in and near the stream channel. The rate coefficient for the oxidation of reduced fulvic acids in the stream (6.5×10^{-3} s^{-1}) is consistent with electron-transfer reactions occurring over short time scales. The significantly larger RI value in the wetland indicates that hyporheic exchange brings reduced fulvic acids from the hyporheic zone into the main stream. The oxidation may either be abiotic, associated with interaction with iron oxides, which may be present in the streambed, or may be biotic as these species can be used as an energy source by bacterial species found in many habitats (*32*). Diminished fulvic acid peaks and differences in RI values between the measured and PARAFAC modeled EEMs of the S3 sample and the conservative transport EEM imply a high reactivity of fulvic acids across the hyporheic zone-stream biogeochemical gradient (Figure 4).

The effects of hyporheic exchange on reactive constituents at the reach scale contribute to patterns seen at the catchment scale data (Figure 5). Given the stable DOC concentrations from ARK to GL4 and the large rate coefficient for the decay of DOC in the stream, the reduced state of the fulvic acids transported into the stream represents an additional energy source for microorganisms living in the oxidized zones of the hyporheic zone or in the stream itself. The observed increase in NO_3^- between ARK and NAV may be explained by the transport of NH_4^+ from the hyporheic zone to the main stream channel where it is rapidly oxidized. The simulations for the decay of NO_3^- and production of NH_4^+ (Figure 3) suggest that NO_3^- is being used as an electron acceptor and/or NH_4^+ is being released through decomposition in the wetland. These processes may be dominant during low flow conditions, as evidenced by the greater contribution of "old" water as the season progresses at both NAV and GL4.

Acknowledgments

We thank C. Johanson for help with Matlab and C. Seibold for chemical analyses. K. Cozetto, J. Joslin, and N. Mladenov provided field assistance. This work was funded by the NSF's LTER Program (grant nos.: DEB-9810218 and OPP-0338299)

Supporting Information Available

Solute transport modeling, reactive transport modeling, and two component mixing model methodologies; Locations of sampling sites (Table S1); Average values of biogeochemical constituents from stream and well sites (Table S2); and Measured EEMs compared with modeled EEMs (Figure S1). This material is available free of charge via the Internet at http://pubs.acs.org.

Literature Cited

(1) Hornberger, G. M; Bencala, K. E.; McKnight, D. M. Hydrological controls on dissolved organic-carbon during snowmelt in the snake river near Montezuma, Colorado. *Biogeochemistry* **1994**, *25* (3), 147−165.

(2) Boyer, E. W.; Hornberger, G. M.; Bencala, K. E.; McKnight, D. M. Response characteristics of DOC flushing in an alpine catchment. *Hydrol. Process.* **1997**, *11*, 1635−1647.

(3) Lewis, W. M.; Grant, M. C. Relationships between snow cover and winter losses of dissolved substances from a mountain watershed. *Arctic Alpine Res.* **1980**, *12(1)*, 11−17.

(4) Baron, J.; McKnight, D. M.; Denning, A. S. Sources of dissolved and particulate organic material in Loch Vale Watershed, Rocky-Mountain-National-Park, Colorado, USA. *Biogeochemistry* **1991**, *15(2)*, 89−110.

(5) McKnight, D. M.; Boyer, E. W.; Westerhoff, P. K.; Doran, P. T.; Kulbe, T.; Andersen, D. T. Spectrofluorometric characterization of dissolved organic matter for indication of precursor organic material and aromaticity. *Limnol. Oceanogr.* **2001**, *46*, 38−48.

(6) Hood, E. W.; McKnight, D. M.; Williams, M. W. Sources and chemical character of dissolved organic carbon across an alpine/subalpine ecotone, Green Lakes Valley, Colorado Front Range, United States. *Water Resour. Res.* **2003**, *39*, 1188, doi:10.1029/2002/WR001738.

(7) Hood, E.; Williams, M. W.; McKnight, D. M. Sources of dissolved organic matter (DOM) in a Rocky Mountain stream using chemical fractionation and stable isotopes. *Biogeochemistry* **2005**, *74(2)*, 231−255.

(8) Hood, E. W.; Williams, M. W.; Caine, N. Landscape controls on organic and inorganic nitrogen leaching across an alpine/subalpine ecotone, Green Lakes Valley, Colorado Front Range. *Ecosystems* **2003**, *6*, 31−45.

(9) Williams, M. W.; Hood, E.; Caine, N. Role of organic nitrogen in the nitrogen cycle of a high elevation catchment, Colorado Front Range. *Water Resour. Res.* **2001**, *37* (10), 2569−2581.

(10) Duff, J. H.; Triska, F. J. Denitrification in sediments from the hyporheic zone adjacent to a small forested stream. *Can. J. Fish. Aquat. Sci.* **1990**, *47*, 1140−1147.

(11) Brookshire, E. N. J.; Valett, H. M.; Thomas, S. A.; Webster, J. R. Coupled cycling of dissolved organic nitrogen and carbon in a forest stream. *Ecology* **2005**, *86* (9), 2487−2496.

(12) Hedin, L. O.; von Fischer, J. C.; Ostrom, N. E.; Kennedy, B. P.; Brown, M. G.; Robertson, G. P. Thermodynamic constraints on nitrogen transformations and other biogeochemical processes at soil-stream interfaces. *Ecology* **1998**, *79* (2), 684−703.

(13) Fulton, J. R.; McKnight, D. M.; Foreman, C.; Cory, R.; Stedmon, C.; Blunt, E. Changes in fulvic acid redox state through the oxycline of a permanently ice-covered Antarctic lake. *Aquat. Sci.* **2004**, *66*, 27−46.

(14) Klapper, L.; McKnight, D. M.; Fulton, J. R.; Blunt-Harris, E. L.; Nevin, K. P.; Lovely, D. R.; Hatcher, P. G. Fulvic acid oxidation state detection using fluorescence spectroscopy. *Environ. Sci. Technol.* **2002**, *36*, 3170−3175.

(15) Cory, R. M.; Mcknight, D. M. Fluorescence spectroscopy reveals ubiquitous presence of oxidized and reduced quinones in dissolved organic matter. *Environ. Sci. Technol.* **2005**, *39*, 8142−8149.

(16) Stedmon, C. A.; Markager, S.; Bro, R. Tracing dissolved organic matter in aquatic environments using a new approach to fluorescence spectroscopy. *Marine Chem.* **2003**, *82*, 239−254.

(17) Scott, D. T.; McKnight, D. M.; Blunt-Harris, E. L.; Kolesar, S. E.; Lovley, D. R. Quinone moieties act as electron acceptors in the reduction of fulvic acids-reducing microorganisms. *Environ. Sci. Technol.* **1998**, *32*, 2984−2989.

(18) Lovley, D. R.; Blunt-Harris, E. L. Role of fulvic acid-bound iron as an electron transfer agent in dissimilatory Fe(III) reduction. *Appl. Environ. Microbiol.* **1999**, *65*, 4252−4254.

(19) Bowman, W. D.; Seastedt, T. R. Structure and function of an alpine ecosystem: Niwot Ridge, Colorado. Oxford University Press: New York, 2001.

(20) Epstein, S.; Mayeda, T. Variations of the $\delta^{18}O$ content of waters from natural sources. *Geochim. Cosmochim. Acta.* **1953**, *4*, 213−224.

(21) Cory, R. M. Redox and photochemical reactivity of dissolved organic matter in surface waters. Ph.D. dissertation, University of Colorado, Boulder, CO, 2005.

(22) Bencala, K. E.; Walters, R. A. Simulation of solute transport in a mountain pool and riffle stream. *Water Resour. Res.* **1983**, *19*, 718−724.

(23) Runkel, R. L. *One-dimensional transport with inflow and storage (OTIS): A solutetransport model for streams and rivers,* U.S. Geological Survey Water Resources. Investigation Report 98-4018; U.S. Geological Survey: Denver, CO, 1998.

(24) Runkel, R. L. A new metric for determining the importance of transient storage. *J. N. Am. Benthol. Soc.* **2002**, *21*, 529−543.

(25) Liu, F.; Williams, M. W.; Caine, N. Source waters and flow paths in an alpine catchment, Colorado Front Range, United States. *Water Resour. Res.* **2004**, *40*, W09401, doi 10.1029/2004WR00307.

(26) Coble, P. G.; Green, S.; Blough, N.; Gagosian, R. Characterization of dissolved organic matter in the Black Sea by fluorescence spectroscopy. *Nature* **1990**, *348*, 432−435.

(27) McKnight, D. M.; Hornberger, G. M.; Bencala, K. E.; Boyer, E. W. In-stream sorption of fulvic acid in an acidic stream: A stream-scale transport experiment. *Water Resour. Res.* **2002**, *38*, 1005, doi. 10.1029/2001WR00269.

(28) Scott, D. T.; Runkel, R. L.; McKnight, D. M.; Voelker, B. M.; Kimball, B. A.; Carraway, E. R. Transport and cycling of iron and hydrogen peroxide in a freshwater stream: Influence of or-

ganic acids. *Water Resour. Res.* **2003**, *39*, 1308, doi:10.1029/2002WR001768.

(29) Wagner, B. J.; Harvey, J. W. Experimental design for estimating parameters of rate limited mass transfer: Analysis of stream tracer studies. *Water Resour. Res.* **1997**, *33*, 1731−1741.

(30) Broshears, R. E.; Bencala, K. E.; Kimball, B. A.; McKnight, D. M. *Tracer-dilution experiments and solute transport simulations for a mountain stream, Saint Kevin Gulch, Colorado*, U.S. Geological Survey Water Resources. Investigations Report 92-4081: U.S. Geological Survey: Denver: CO, 1993.

(31) Peterson, B. J.; Wollheim, W. M.; Mulholland, P. J.; Webster, J. R.; Meyer, J. L.; Tank, J. L.; Martin, E.; Bowden, W. B.; Valett, M. H.; Hershey, A. El; Mcdowell, W. H.; Dodds, W. K.; Hamilton, S. K.; Gregory, S.; Morrall, D. D. Control of nitrogen export from watersheds by headwater streams. *Science* **2001**, *292*, 86−90.

(32) Coates, J. D.; Ellis, D. J.; Blunt-Harris, E. L.; Gaw, C. V.; Roden, E. E.; Lovley, D. R. Recovery of fulvic acid-reducing bacteria from a diversity of environments. *Appl. Environ. Microbiol.* **1998**, *64*, 1504−1509.

Received for review March 17, 2006. Revised manuscript received June 23, 2006. Accepted July 21, 2006.

ES060635J